

Analytical and experimental studies for deformation of circular plates subjected to blast loading[†]

Hashem Gharababaei^{1,*}, Abolfazl Darvizeh^{1,2} and Mansour Darvizeh¹

¹Department of Mechanical Engineering, Engineering Faculty, University of Guilan, P.O. Box 3756, Rasht, Iran

²Department of Mechanical Engineering, Engineering Faculty, Islamic Azad University of Bandar Anzali, Anzali, Iran

(Manuscript Received September 22, 2009; Revised March 31, 2010; Accepted April 23, 2010)

Abstract

In this paper, experimental responses of the clamped mild steel, copper, and aluminum circular plates subjected to blast loading are investigated. Extensive experimental results concerning variations of central deflection are presented. Approximate energy analysis is used for the analytical modeling of the mid-point deflection thickness ratio of the circular plates. The essence of the model is to describe the deformation profile, which depends on the distribution of impulsive load. By using the present modeling, one can show how the mid-point deflection varies with the variations of the important parameters. The results obtained from the present model show very good agreement with the experimental data.

Keywords: Analytical modeling; Circular plate; Deformation; Experimental test; Impulsive load

1. Introduction

Solid phase-based forming has attracted a great amount of interest as a new technology of forming since it can compensate for the disadvantages of conventional forming processes. However, it still has difficulties in industrial production due to problems such as the reheating of the billet, high manufacturing costs, and an inability to produce large parts [1].

In sheet metal forming, the amount of deformation has always attracted immense experimental and analytical research efforts. The amount of deformation is limited by the occurrence of plastic instability in the form of localized necking or wrinkling. The localized necking is a very important phenomenon in determining the optimum deformation that can be imposed on a work piece [2]. The prediction of fractures in metal forming is very useful for evaluating the feasibility of a forming process. Many ductile fracture criteria have been proposed over the past years for the prediction of fractures, particularly in cases where the fracture occurs without the formation and development of necking [3].

High rate metal forming processes were fairly well developed. These techniques had some advantages over conventional metal forming. These include the ability to use single-sided dies, reduced spring back, and improved formability [4].

One widely considered structural problem is that of a fully-clamped metallic circular plate subjected to transverse impulsive loads. Nurick and Martin have carried out some studies of the behavior of such plates subjected to blast loading [5, 6]. Experimental studies concerning the response of metal plates under blast loading have also been the subject of a great deal of research. Up to 1989, much of the research has concentrated on the response of the plates under uniform distribution of impulsive loading over the area of the plate [5].

In subsequent years, the response of mild steel plates to a central localized blast load has been studied experimentally [6-10]. Experimental works on structures under explosive loading were performed in order to measure large inelastic deformation (mode I), tensile tearing (mode II) and transverse shear rapture (mode III). These failure modes were first defined for beams in reference [11]. Subsequently, these modes were observed for circular and square plates [9, 12].

It was reported that permanent mild point deflection increased with increasing impulse. As impulse increased, the failure observed in the plates passed from mode I to mode II and tended towards mode III at the highest impulses [9]. It was reported in reference [7] that localized blast loading on clamped circular steel plates resulted in deformations characterized by an inner dome at top of large global dome. At higher impulses, thinning and tearing in the central region and also thinning at the plate boundary were observed. At the highest impulses caps were torn away from the plate, and it was reported in reference [13] that residual velocity of the cap

[†] This paper was recommended for publication in revised form by Associate Editor Chang-Wan Kim

*Corresponding author. Tel.: +92 131 6690270, Fax: +92 131 6690271

E-mail address: ghababaei@guilan.ac.ir, hghbabaei@yahoo.com

© KSME & Springer 2010

increased with increasing impulse. All of the works given in references [6-10, 13] on localized loading were performed using plastic explosive sited 13mm away from the plate structure. The reason for using a polystyrene pad is to prevent spalling of the incident face. In the work reported in reference [10], a blast tube has been employed with the explosive distanced away from the plate. The effect of stand-off distance was considered and it was demonstrated that the response of the plate was affected by increasing the stand-off distance. A new dimensionless impulse term which incorporates the effect of stand-off distance was proposed in reference [10].

An understanding of the response of structures when subjected to dynamic loads that produce large inelastic and plastic deformations and damage is important in solving a variety of engineering problems. Despite significant progress been made in this field during the past decade, complete theoretical analysis of the dynamic structural response is still a formidable task, even for very simple structures such as beams and plates [14]. Recently, various simplified models have been developed for predicting the dynamic response of circular plate structures to intense blast loads. More recently, Wen *et al.* developed a quasi-static procedure to predict the deformation and failure of a clamped beam struck transversely at any point by a mass traveling at low velocities [15]. A similar procedure has been proposed in references [15-18] to construct failure maps for fully clamped metal beams and circular plates under impulsive loadings using a hybrid model (i.e., r.p.p. for the bending-membrane solution and a power law for the effects of local shear).

This paper presents experimental and analytical results on mild steel, copper, and aluminum circular plates subjected to blast loading. The aim of the experimental study is to investigate the effect of stand-off distance, plate thickness and material properties on mid-point deflection. Analytical study provides a simple theoretical formulation for predicting high rate plastic deformation of circular plates subjected to transverse impulsive loading. The analytical models obtained in this work respect to other models already reported in literature have good agreement with the experimental results.

2. Experimental tests

2.1 Experimental procedure

The test specimens were 200mm by 200mm and varied in thickness from 1.6 mm to 3.0 mm. Plate specimens were not subjected to heat treatment before being used in blast loading condition. The specimens were clamped in a frame, comprising of two (200mm × 200 mm) frames made from 20mm thick mild steel plating. Two stand-off distances were employed to vary the spatial uniformity of the loading – 50 mm and 300 mm. A tube of required length was screwed into the front clamp; the back frame had a 100 mm diameter hole (the same as the internal tube diameter). Each specimen had a circular exposed area with a diameter of 100 mm. Plastic explosive (PE4) was molded into the appropriate charge diameter disc

and sited at the open end of the blast tube, as shown in Fig. 1. 1.g leader of explosive was used to attach the detonator to the main charge, making the total mass of the explosive the sum of the disc and the 1.g leader. The total charge masses range from 2.g to 19.g, with the stand-off distance being equal to the length of the attached tube. The blast loading was generated by electrical detonation of the explosive charge allowing the resulting blast wave to travel down the blast tube and impinge upon the target plate. The experimental details are given in Table 1. The test rig, complete with clamping frames and tube, was mounted onto a ballistic pendulum. The oscillation amplitude of the swing pendulum was used to determine the impulse imparted to the plates. Photographs corresponding to experimental set-up and the deformed plate are given in Figs. 2 and 3, respectively. [19]

All tests were performed at room temperature (20°C). Immediately after each test, it was found by direct observation that the temperature change of the blast loaded specimen was not significant. This might be due to very fast expansion of gaseous products generated by the explosion and very short duration of interaction between pressure pulse and target plate. It is a common practice to assume that input energy provided by explosive pressure is converted into plastic work and kinetic energy during high rate deformation of the plate.

Table 1. Details of experiments.

| Parameters | Details |
|--------------------------|-------------------------|
| Plate material | Steel, Copper, Aluminum |
| Plate diameter (mm) | 100 |
| Plate thickness (mm) | 1.6, 2.0, 3.0 |
| Stand-off distance (mm) | 50, 300 |
| Charge diameter (mm) | 20, 33 |
| Range of charge mass (g) | 2-19 |

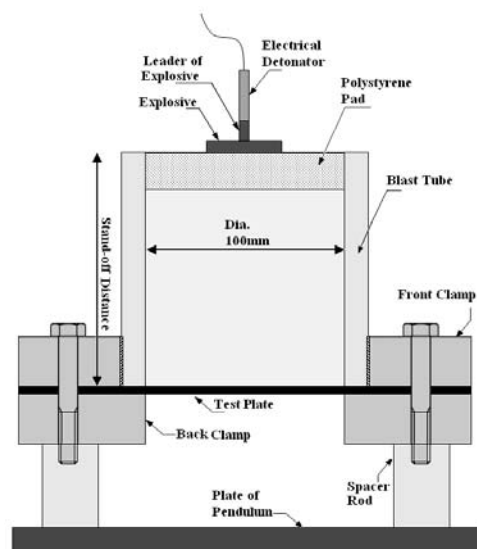
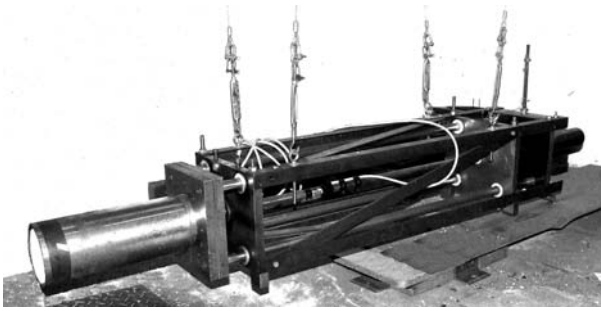
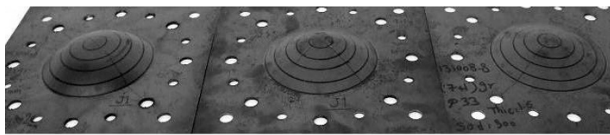


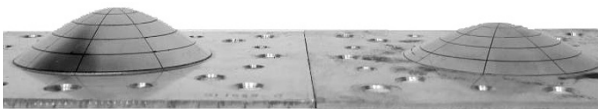
Fig. 1. Schematic of the experimental test rig.

Fig. 2. Photograph of experimental arrangement.¹

(a) Steel plates



(b) Copper plates



(c) Aluminum alloy plates

Fig. 3. Photographs of typical blast loaded plates.

2.2 Mechanical properties of the plate materials

Tensile test specimens were prepared from commercially pure (99.5%) copper, aluminum alloy 1200-H4, and mild steel with different thicknesses. To include the effect of anisotropy on the values of yield stress, two specimens were cut from each sheet in longitudinal and transverse directions. The results of tensile test on specimens cut longitudinally show no significant difference from those cut transversely.

The mean average values of yield stress and ultimate tensile stress are calculated for each material at different thicknesses. A summary of the properties of the different plate materials is given in Table 2. It is evident from Table 2 that mild steel has the highest yield stress, followed by copper, then aluminum alloy 1200-H4. The yield stresses of the steel and aluminum alloys were approximately constant over the thickness range. The 2 mm thick copper was much stronger than the 3 mm thick copper; this could be due to the initial work hardening.

It is assumed that input energy generated by blast is converted into plastic work and kinetic energy during the high rate deformation process. The effect of temperature on material behavior has been neglected since the temperature dependency of material may introduce a complex problem. To

¹ The experimental arrangement had been provided by Prof. G. N. Nurick from the University of Cape Town

Table 2. Summary of tensile test results on steel, copper and aluminum.

| Material | ρ Density (Kg/m ³) | Nominal Thickness (mm) | Yield Stress ² (MPa) |
|-------------------------|-------------------------------------|------------------------|---------------------------------|
| Steel | 7800 | 1.6, 2, 3 | 318 |
| Copper | 8940 | 2 | 277 |
| | | 3 | 201 |
| Aluminium Alloy 1200 H4 | 2700 | 2, 3 | 120 |

include the effect of strain rate in dimensionless analysis, the dynamic yield stress was calculated.

The resistance to through thickness thinning is measured by R_{wt} , which is defined as the plastic strain ratio of width to thickness in a sheet. R_{wt} measures the normal anisotropy. Also, resistance to yielding increases with increased R_{wt} due to enlargement of the yield surface. Immediately after detonation of the explosive charge, a pressure pulse of impulsive nature and with very high intensity interacts with the plate through thickness direction. The intensity of the shock pressure is far greater than the mechanical strength of the plate in any direction. Hence, the effect of normal anisotropy is not included.

2.3 Experimental results and discussion

For the first set of tests, the stand-off distance was held constant at 50mm and 300mm respectively, for each material and three different thicknesses, the effect of impulse values was investigated. By comparison of Figs. 4(a), 4(b) and 4(c) the profile of the plates tested at the 50mm stand-off distance was observed to be more conical than those plates tested at the 300mm stand-off distance. This effect might be due to the reduction of the stand-off distance. The effect of the explosion upon the central portion of the plate becomes increasingly greater relative to the distance of outer edges and increasingly smaller relative to the angle of incident between the impulsive pressure wave and the plate at the outer edges. Impulse values were increased from those causing only a slight deformation to an amount sufficient to produce rupture. The experimental data and results are presented in Table 3. The charge masses listed include the 1.g leader charge attached to detonator.

3. Analytical solution

The distribution of the blast load depends on the stand-off distance between the explosive charge and the target plate. At a stand-off distance less than the plate radius, the blast load is considered to be localized and deflection profiles take a conical form. For a stand-off distance greater than the plate radius, the load is considered uniformly distributed over the entire plate area and deflection profiles are similar to global dome. Photographs of deformed plates with two different loading distributions are shown in Fig. 4.

² For copper and aluminum, there is no well defined yield point and the 0.2% proof stress is listed instead.

Table 3. Results of blast loading tests.

| Plate material ³ | plate Thickness (mm) | Charge mass (g) | Diameter charge (mm) | Stand-off distance (mm) | Impulse (Ns) | Mid-point deflection (mm) | Failure mode |
|-----------------------------|----------------------|-----------------|----------------------|-------------------------|--------------|---------------------------|--------------|
| St | 1.6 | 5 | 33 | 300 | 13.02 | 11.28 | I |
| St | 1.6 | 6 | 33 | 300 | 13.69 | 11.36 | I |
| St | 1.6 | 8 | 33 | 300 | 17.08 | 13.72 | I |
| St | 1.6 | 10 | 33 | 300 | 20.28 | 16.5 | I |
| St | 1.6 | 12 | 33 | 300 | 25.07 | 20 | I |
| St | 1.6 | 13 | 33 | 300 | 25.96 | 20.2 | I |
| St | 1.6 | 14 | 33 | 300 | 27.5 | 22.5 | I |
| St | 1.6 | 6 | 33 | 50 | 12.82 | 15.46 | I |
| St | 1.6 | 10 | 33 | 50 | 19.66 | 21.6 | I |
| St | 1.6 | 12 | 33 | 50 | 22.56 | --- | II |
| St | 2 | 5 | 33 | 300 | 12.46 | 8.6 | I |
| St | 2 | 6 | 33 | 300 | 13.6 | 9.58 | I |
| St | 2 | 8 | 33 | 300 | 18.18 | 12 | I |
| St | 2 | 10 | 33 | 300 | 20.55 | 13.67 | I |
| St | 2 | 13 | 33 | 300 | 25.5 | 17.37 | I |
| St | 2 | 13 | 33 | 300 | 26.12 | 16.7 | I |
| St | 2 | 16 | 33 | 300 | 30.74 | 19.08 | I |
| St | 2 | 6 | 33 | 50 | 12 | 11.73 | I |
| St | 2 | 10 | 33 | 50 | 19.36 | 18.24 | I |
| St | 2 | 13 | 33 | 50 | 23.78 | 21.5 | I |
| St | 2 | 15 | 33 | 50 | 26.34 | --- | II |
| St | 3 | 5 | 33 | 300 | 11.78 | 3.55 | I |
| St | 3 | 6 | 33 | 300 | 12.75 | 3.22 | I |
| St | 3 | 8 | 33 | 300 | 18.23 | 6.83 | I |
| St | 3 | 10 | 33 | 300 | 20.4 | 6.66 | I |
| St | 3 | 13 | 33 | 300 | 26.11 | 10.01 | I |
| St | 3 | 13 | 33 | 300 | 26.5 | 10.62 | I |
| St | 3 | 15 | 33 | 300 | 28.75 | 11.56 | I |
| St | 3 | 6 | 33 | 50 | 11.39 | 7.28 | I |
| St | 3 | 10 | 33 | 50 | 19.57 | 13.17 | I |
| St | 3 | 13 | 33 | 50 | 25.09 | 14 | I |
| Cu | 2 | 4 | 33 | 50 | 9.35 | 9.82 | I |
| Cu | 2 | 7 | 33 | 50 | 15.04 | 16.11 | I |
| Cu | 2 | 10 | 33 | 50 | 19.22 | 22.18 | I |
| Cu | 2 | 13 | 33 | 50 | 24.1 | 25.97 | I |
| Cu | 2 | 14 | 33 | 50 | 26.4 | --- | II |
| Cu | 2 | 3 | 33 | 50 | 5.19 | 5.4 | I |
| Cu | 2 | 6 | 33 | 50 | 13.99 | 14.9 | I |
| Cu | 2 | 9 | 33 | 50 | 19.34 | 20 | I |
| Cu | 2 | 5 | 20 | 50 | 8.46 | 9.43 | I |
| Cu | 2 | 8 | 20 | 50 | 12.47 | 13.68 | I |
| Cu | 2 | 11 | 20 | 50 | 17.04 | 17.23 | I |
| Cu | 2 | 6 | 33 | 300 | 13.98 | 13 | I |
| Cu | 2 | 8 | 33 | 300 | 18.18 | 16.34 | I |
| Cu | 2 | 10 | 33 | 300 | 21.02 | 18.25 | I |
| Cu | 2 | 5 | 33 | 300 | 12.6 | 10.85 | I |
| Cu | 2 | 7 | 33 | 300 | 17.25 | 14.63 | I |
| Cu | 2 | 9 | 33 | 300 | 20.7 | 17.6 | I |
| Cu | 2 | 11 | 33 | 300 | 24.8 | 20.67 | I |
| Cu | 2 | 13 | 33 | 300 | 28.6 | --- | II |
| Cu | 3 | 5 | 33 | 300 | 12.39 | 7.52 | I |
| Cu | 3 | 9 | 33 | 300 | 19.13 | 11.85 | I |
| Cu | 3 | 13 | 33 | 300 | 25.61 | 15.46 | I |
| Cu | 3 | 16 | 33 | 300 | 30.2 | 18.12 | I |

³ St: steel, Cu: copper, Al: Aluminium

Table 3. Continued.

| Plate material | plate Thickness (mm) | Charge mass (g) | Diameter charge (mm) | Stand-off distance (mm) | Impulse (Ns) | Mid-point deflection (mm) | Failure mode |
|----------------|----------------------|-----------------|----------------------|-------------------------|--------------|---------------------------|--------------|
| Cu | 3 | 19 | 33 | 300 | 34.63 | 21.2 | I |
| Cu | 3 | 13 | 33 | 300 | 26.46 | 15.88 | I |
| Cu | 3 | 4 | 33 | 50 | 10.25 | 7.6 | I |
| Cu | 3 | 7 | 33 | 50 | 14.22 | 11.24 | I |
| Cu | 3 | 10 | 33 | 50 | 19.55 | 16.4 | I |
| Cu | 3 | 13 | 33 | 50 | 22.98 | 18.97 | I |
| Cu | 3 | 16 | 33 | 50 | 27.82 | --- | II |
| Al | 2 | 2 | 33 | 300 | 5.16 | 8.6 | I |
| Al | 2 | 3 | 33 | 300 | 8.25 | 14.9 | I |
| Al | 2 | 4 | 33 | 300 | 10.82 | 24.22 | I |
| Al | 2 | 4.5 | 33 | 300 | 12.32 | 26.3 | I |
| Al | 2 | 3.5 | 33 | 300 | 9 | 21 | I |
| Al | 2 | 5 | 33 | 300 | 14.1 | --- | II |
| Al | 2 | 2 | 33 | 50 | 2.72 | 7.35 | I |
| Al | 2 | 3 | 33 | 50 | 3.91 | 11.4 | I |
| Al | 2 | 4 | 33 | 50 | 8.62 | 23.3 | I |
| Al | 2 | 2.5 | 20 | 50 | 4.92 | 15.24 | I |
| Al | 2 | 3.5 | 20 | 50 | 7.44 | 19.04 | I |
| Al | 2 | 4.5 | 33 | 50 | 9.75 | --- | II |
| Al | 3 | 4 | 33 | 300 | 9.72 | 14.1 | I |
| Al | 3 | 5 | 33 | 300 | 13.71 | 19.9 | I |
| Al | 3 | 6 | 33 | 300 | 14.96 | 21.9 | I |
| Al | 3 | 7 | 33 | 300 | 16.2 | --- | II |
| Al | 3 | 3 | 33 | 50 | 2.72 | 5.4 | I |
| Al | 3 | 4 | 33 | 50 | 10.84 | 15.97 | I |
| Al | 3 | 5 | 33 | 50 | 11.54 | 22.9 | I |
| Al | 3 | 4.5 | 33 | 50 | 9.65 | 17.21 | I |
| Al | 3 | 4 | 20 | 50 | 7.28 | 14.56 | I |
| Al | 3 | 5 | 20 | 50 | 9.28 | 16.88 | I |
| Al | 3 | 6 | 20 | 50 | 10.2 | 21 | I |
| Al | 3 | 7 | 20 | 50 | 11.91 | 21.6 | I |
| Al | 3 | 6 | 33 | 50 | 12.8 | --- | II |

3.1 Localized distribution of load ($0 \leq \text{Stand-off} \leq R$)

In this case, the displacement profile of an impulsively loaded circular plate up to initial rupture takes the approximate conical form. Thus, based on experimental observation, a suitable mathematical function to describe this type of deflection profile is the zero-order Bessel function of the first kind as [19]:

$$w(r) = W_0 J_0 \left(\frac{a.r}{R} \right) \tag{1}$$

where $w(r)$ is transverse displacement of the plate and W_0 is transverse displacement at the center. r and R are the radial coordinate and outer radius of the plate, respectively. a is 1st root of J_0 and its value is 2.4048.

The plastic work done during the deformation of the plate is:

$$W_P = \int_V (\sigma_r \epsilon_r + \sigma_\theta \epsilon_\theta) dV. \tag{2}$$

It is assumed that radial and circumferential strains are significant and thickness strain ϵ_t is negligible. According to theoretical relations for radial and circumferential strains, which are available in reference [18], and by using Eq. (1), the function of strains can be obtained.

Furthermore, it is assumed that the mean dynamic flow stress can be expressed as a scalar multiple of the quasistatic yield stress.

$$\sigma_d = \lambda \sigma_y \tag{3}$$

where σ_d is the mean dynamic flow stress, λ is a constant, and σ_y is the quasi-static yield stress.

For a hydrostatic pressure-insensitive material such as metals, the hydrostatic component of the stress tensor does not have significant influence on yielding and plastic flow. Therefore, these components can be subtracted from the stress tensor, and it is common practice to employ the Tresca or Von-Mises yield criterion and VonMises flow rules. Introducing Tresca yield criterion and VonMises flow relation for the rigid plastic material, the following relation can be obtained for the circular plate

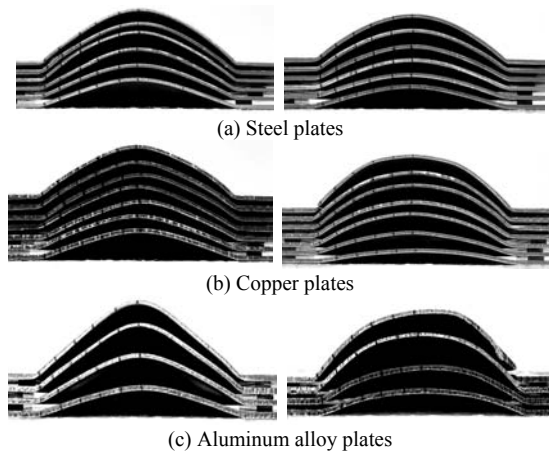


Fig. 4. Photographs of the deformation profiles of blast loaded plates (at two different stand-off distance, Lh: 50mm and Hh: 300mm).

$$\sigma_r = \sigma_\theta = \sigma_d \tag{4}$$

Eq. (2) can be converted into the following equation:

$$\begin{aligned} W_p &= \int_V \lambda \sigma_y (\epsilon_r + \epsilon_\theta) dV \\ &= \int_0^R \int_{-H/2}^{H/2} \lambda \sigma_y (\epsilon_r + \epsilon_\theta) 2\pi r dz dr \end{aligned} \tag{5}$$

where H is the thickness of the plate and z is the transverse coordinate. It should be noted that the direction of principle stresses and principle strains are the same. Substituting the relevant values into Eq. (5) and integrating with respect to z and r gives:

$$W_p = \frac{1}{2} \pi \lambda \sigma_y [H(aJ_1(a)W_o)^2 + H^2 aJ_1(a)W_o] \tag{6}$$

The energy dissipated through plastic work is equal to the initial kinetic energy of the plate. According to the principle of momentum conservation, induced initial velocity by the impulsive load is:

$$V_o = \frac{I}{m}, \tag{7}$$

$$E_k = \frac{1}{2} m V_o^2 = \frac{I^2}{2m}, \quad \text{where } (m = \rho \pi R^2 H) \tag{8}$$

where ρ is the density, V_o and m are the initial impulsive velocity and the mass of plate, respectively, and E_k is kinetic energy imparted by an input impulse I to the plate. Equating Eqs. (6) and (8) gives:

$$W_o = \frac{\sqrt{(HaJ_1(a))^2 + 4 \cdot \frac{(I a J_1(a))^2}{(\pi R H)^2 \lambda \rho \sigma_y}} - HaJ_1(a)}{2(aJ_1(a))^2} \tag{9}$$

Introducing ϕ as a dimensionless impulsive parameter

$$\phi = \frac{I}{\pi R H^2 \sqrt{\rho \sigma_y}}, \tag{10}$$

Eqs. (9) and (10) lead to the expression for the relationship between the mid-point deflection – thickness ratio (dimensionless displacement) and dimensionless impulse parameter.

$$\frac{W_o}{H} = \frac{\sqrt{1 + \frac{4}{\lambda} \phi^2} - 1}{2(aJ_1(a))} \tag{11}$$

3.2 Uniform distribution of load (Stand-off > R)

For a stand-off distance greater than the radius of the test specimen, the deformation profile does not have a conical form resembling a large global dome. Based on experimental observation, the following formula is chosen to describe the deformation [19].

$$w(r) = W_o \left(1 - \left(\frac{r}{R} \right)^\alpha \right) \tag{12}$$

where $w(r)$ is transverse displacement of the plate and W_o is transverse displacement at the center. r and R are the radial coordinate and outer radius of plate, respectively. α is the order of the profile function. According to test results, the value of α can be assumed 2, but for aluminum plates, deformation profiles resemble a global dome, so in this case the order of profile function is different and appropriate value of α is 3.

Upon integration the dissipated plastic work is:

$$W_p = \frac{1}{2} \pi \lambda \sigma_y \alpha (H W_o^2 + H^2 W_o) \tag{13}$$

Equating plastic work with kinetic energy imparted by an input impulse I to the plate, Eq. (8), and considering dimensionless impulsive parameter, Eq. (10), leads to the following expression for the relationship between the mid-point deflection thickness ratio and dimensionless impulse parameter

$$\frac{W_o}{H} = \frac{1}{2} \left(\sqrt{1 + \frac{4}{\lambda \alpha} \phi^2} - 1 \right) \tag{14}$$

4. Material model

For determining the value of λ , the ratio between static and dynamic yield stresses, the well-known Cowper–Symonds constitutive equation is used. Therefore, Eq. (3) can be rewritten in the form:

$$\frac{\sigma_d}{\sigma_y} = \lambda = 1 + \left(\frac{\dot{\epsilon}_m}{D} \right)^{\frac{1}{q}} \tag{15}$$

Table 4. Summary of material constants in Eq. (15) for steel, copper and aluminum.

| Material | D (s ⁻¹) In Eq. (15) | q In Eq. (15) | λ For uniform load | λ For localized load |
|----------------------------|-------------------------------------|------------------|--------------------------|----------------------------|
| Steel | 40.4 [20] | 5.0 [20] | 3.08 | 2.8 |
| Copper | 720 [21] | 1.56 [21] | 2.65 | 2.01 |
| Aluminium Alloy 1200 H4 | 6500 [20] | 4.0 [20] | 1.87 | 1.6 |

where $\dot{\epsilon}_m$ is the mean strain rate and D and q are material constants. The constant values for mild steel, copper, and aluminum are given in Table (4). [20, 21]

As an estimate of mean strain rate $\dot{\epsilon}_m$, taking a moderate value for deflection of 15 mm, functions of radial strain imply a maximum strain of approximately 0.089 for localized distribution of load and 0.19 ($\alpha=2$) or 0.45 ($\alpha=3$) for uniform distribution of load. Bodner, Symonds and Nurick reported in references [22, 23] that blast loaded plates reach their maximum deflection in approximately 120 μ s, which implies a mean strain rate in the order of 742s⁻¹ for localized distribution of load and 1583s⁻¹ ($\alpha=2$) and 3750s⁻¹ ($\alpha=3$) for uniform distribution of load. Substituting the values for the mean strain rate and material constants into Eq. (15) yields an average value for λ . For each type of material and distribution of load, values of λ are given separately in Table 4. While this is merely an estimate, it shows that the value of λ required to correlate the analytical and experimental results are reasonable [24].

5. Comparison of the experimental and analytical results

The results obtained from analytical models in the proceeding section, Eqs. (11) and (14), are compared with the different set of experimental results which are presented in Table 3. Fig. 5 Shows the comparison between the theoretical prediction of the mid-point deflection thickness ratio [using Eq. (11)] and the experimental values for different materials under the localized distribution of impulsive load, created with a stand-off distance of 50 mm. It is clear from Fig. 5 that the results obtained from the model are in good agreement with the experimental results. Similarly, Fig. 6 shows the comparison between predictions of Eq. (14) and the experimental values in the case of uniform distribution of blast load, created with a stand-off distance of 300 mm. The results of this model are also in good correlation with the experimental ones.

To further validate the prediction of the analytical models for the cases of localized and uniform distribution of loads, mid-point deflection thickness ratio versus dimensionless parameter ϕ are plotted for different materials [see Figs. 7-9]. From these figures it is evident that the proposed model can be successfully used to predict the mid-point deflection thickness ratio for different materials under conditions of localized and uniform distribution of impulsive loads.

There have been many research efforts for theoretically mod-

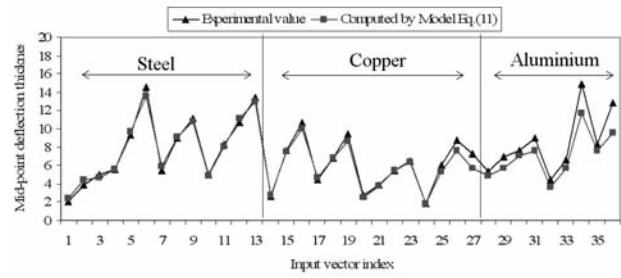


Fig. 5. Graph comparing predicted and value of measured mid-point deflection–thickness ratio in the case of localized load.

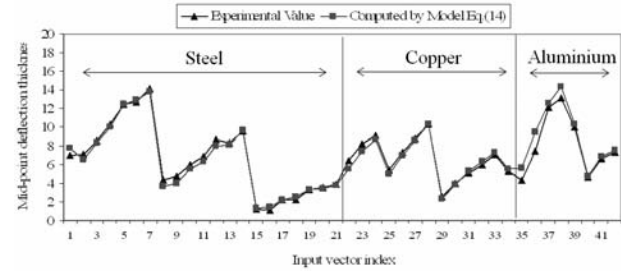


Fig. 6. Graph comparing predicted and value of measured mid-point deflection–thickness ratio in the case of uniform load.

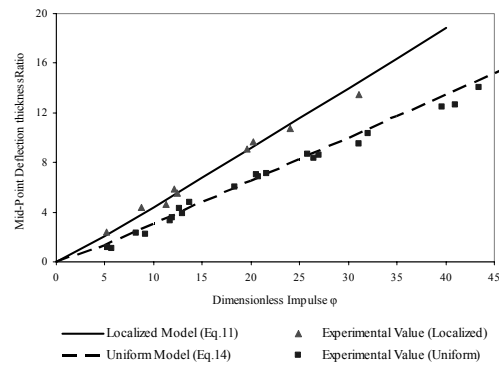


Fig. 7. Graph of mid-point deflection thickness ratio versus dimensionless number (ϕ) for steel plate subjected to localized and uniform impulsive loads.

eling the dynamic response and deformation of thin plates to predict the relationship of deflection-thickness ratio as a function of impulse, plate geometry and material properties [5, 10, 19, 25]. These models predict maximum mid-point deflection of circular plates for uniform and localized loads and are summarized in Table 5. For the comparison, Table 6 also depicts RMSE⁴ of the model equations which are referenced in Table 5 and those obtained from present model Eqs. (11) and (14). Evidently, it can be observed that the models obtained in this paper have less RMSE compared with that of other models reported in Table 5. However, RMSE of models in reference [19] are low and their accuracy is similar to obtained models in this work, though equation of these models is too complex.

⁴ Root Mean Square Error

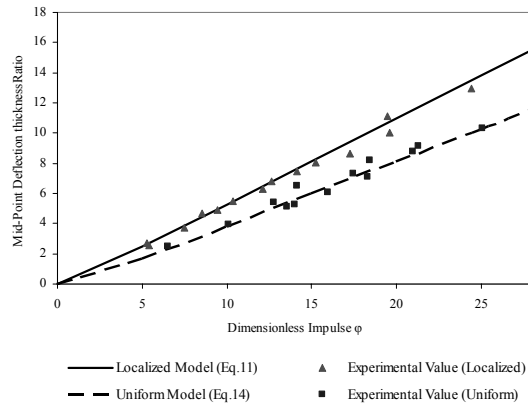


Fig. 8. Graph of mid-point deflection thickness ratio versus dimensionless number (ϕ) for copper plate subjected to localized and uniform impulsive loads.

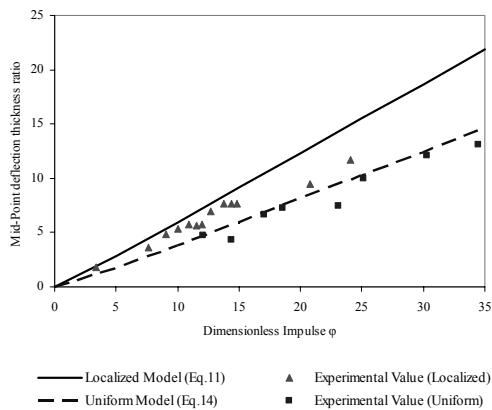


Fig. 9. Graph of mid-point deflection thickness ratio versus dimensionless number (ϕ) for aluminum plate subjected to localized and uniform impulsive loads.

6. Conclusion

This paper reports the results of the experimental observations from an extensive series of blast tests and presents the analytical analysis on clamped circular plates subjected to different distribution of impulsive loading.

The experimental results represent the behavior of ferrous and non-ferrous metal plates and provide an insight to predict the relationship between mid-point deflections and applied impulsive load. Also, the obtained results show the importance of material properties, stand-off distance and plate thickness on the deformation profiles.

From the present analytical modeling carried out in the present research work, the prediction of central deflection of the plate subjected to impulsive loading might be found more accurately. This can be shown by comparing the obtained analytical results with those from other research workers and experimental ones. The error is less than those obtained from other models already reported in literature. Yet it is intended that this analytical approach will be complementary to existing ones. However, the current establishment of equations in the present models is more straightforward.

Table 5. Equations of mid-point deflection-thickness ratio of thin circular plates subjected to impulsive load.

| References | Equations |
|--|---|
| Hudson [5] | $\frac{W_c}{H} = \frac{0.318I}{t^2 R(\rho\sigma_0)^{1/2}}$ |
| Symonds & Wierzbicki [5] | $\frac{W_c}{H} = \frac{0.212I}{t^2 R(\rho\sigma_0)^{1/2}}$ |
| Lipman [5] | $\frac{W_c}{H} = \frac{0.132I}{t^2 R(\rho\sigma_0)^{1/2}}$ |
| Jones [5] | $\frac{W_c}{H} = \frac{0.260I}{t^2 R(\rho\sigma_0)^{1/2}}$ |
| Batra & Dubey [5] | $\frac{W_c}{H} = \frac{0.382I}{t^2 R(\rho\sigma_0)^{1/2}}$ |
| NurickMartin (model (1)) [5] | $\frac{W_c}{H} = \frac{0.135I}{t^2 R(\rho\sigma_0)^{1/2}}$ |
| Nurick & Martine (model (2)) [5] | $\frac{W_c}{H} = \frac{0.318I}{t^2 R(\rho\sigma_0)^{1/2}} \left(1 + Ln \left(\frac{R}{R_0} \right) \right)$ |
| Gharababaei, Nariman zadeh and Darvizeh [25] | $\frac{W_c}{H} = \frac{0.12I}{t^2 R(\rho\sigma_0)^{1/2}} \left(\frac{R}{R_0} \right)$ |
| Nurick & Jacob [10] | $\frac{W_c}{H} = \frac{0.425I}{\pi t^2 R(\rho\sigma_0)^{1/2}} \left(\frac{1 + \ln \left(\frac{R}{R_0} \right)}{1 + \ln \left(\frac{S}{R_0} \right)} \right)$ |
| Gharababaei and Darvizeh [19] | Eq. (29) for localized load Eq. (40) for uniform load |

Table 6. Root mean squares of errors (RMSE) of various models for the experimental data which is referenced in Table 5.

| Models | RMSE | |
|--|--------------------------------|------------------------------|
| | Localized distribution of load | Uniform distribution of load |
| Hudson [5] | 7.99 | 14.53 |
| Symonds & Wierzbicki [5] | 2.9219 | 7.208 |
| Lipman [5] | 1.1985 | 1.833 |
| Jones [5] | 5.208 | 10.523 |
| Batra & Dubey [5] | 11.078 | 18.977 |
| Nurick & Martin (model (1)) [5] | 1.0789 | 2.017 |
| Nurick & Martine (model (2)) [5] | 26.96 | 39.0 |
| Gharababaei, Nariman zadeh and Darvizeh [24] | 13.69 | 17.7 |
| Nurick & Jacob [10] | 1.065 | 2.645 |
| Gharababaei and Darvizeh [19] | 0.9968 | 0.605 |
| Model (Eq.11) | 0.9917 | ----- |
| Model (Eq.14) | ----- | 0.5607 |

Acknowledgements

The authors express their thanks to Prof. G. N. Nurick, Dr. G. S. Langdon and Mr. T. J. Cloete for their help with the experiments and for machining the modified ballistic pendulum. The authors also wish to thank all of member of BISRU group at the University of Cape Town.

Nomenclature

| | |
|--------------------|--|
| W | : Transverse displacement of plate |
| W_o | : Transverse displacement of plate at center |
| r | : Radial coordinate |
| R | : Radius of plate |
| J_o | : Zero-order Bessel function |
| a | : 1 st root of J_o |
| J_1 | : First-order Bessel function |
| ϵ_r | : Radial strain |
| ϵ_θ | : Circumferential strain |
| ϵ_t | : Thickness strain |
| z | : Transverse coordinate |
| W_p | : Plastic work done |
| σ_r | : Radial stress |
| σ_θ | : Circumferential stress |
| σ_d | : Mean dynamic stress |
| λ | : Constant defined in Eq. (3) |
| σ_y | : Quasi-static yield stress |
| H | : Plate thickness |
| ρ | : Density of plate material |
| E_k | : Kinetic energy |
| I | : Input impulse |
| V_o | : Initial impulsive velocity |
| m | : Mass of plate |
| φ | : Dimensionless impulsive |
| ϵ_m° | : Mean strain rate |
| D | : Material constant, defined in Eq. (15) |
| q | : Material constant, defined in Eq. (15) |
| V | : volume of plate |
| α | : order of profile function |
| R_o | : Radius of explosive |
| S | : Stand-off distance |

References

- [1] T. W. Kim, H. H. Kim, J. W. Bae, S. M. Lee and C. G. Kang, Semi-solid die forging of Al6061 wrought aluminium alloy with electromagnetic stirring, *Proc IMechE, Part B: J. Engineering Manufacture*, 222 (B9) (2008) 1083-1095.
- [2] R. Safikhani, R. Hashemi and A. Assempour, The strain gradient approach for determination of forming limit stress and strain diagrams. *Proc IMechE, Part B: J. Engineering Manufacture*, 222 (B4) (2008) 467-483.
- [3] T. Zheng, S. H. Zhang, D. Sorgente, L. Tricarico and G. Palumbo, Approach of using a ductile fracture criterion in deep drawing of magnesium alloy cylindrical cups under non-isothermal condition. *Proc IMechE, Part B: J. Engineering Manufacture*, 221 (B6) (2007) 981-986.
- [4] M. Gerdooei and B. M. Dariani, Strain-rate-dependent forming limit diagrams for sheet metals, *Proc IMechE, Part B: J. Engineering Manufacture*, 222 (B12) (2008) 1651-1659.
- [5] G. N. Nurick and J. B. Martin, Deformations of thin plates subjected to impulsive loading - a review; Part I - Theoretical considerations. *Int. J. Impact Eng.*, 8 (2) (1989) 159 - 170.
- [6] G. N. Nurick and J. B. Martin, Deformation of thin plates subjected to impulsive loading - a review; Part II - Experimental studies. *Int. J. Impact Eng.*, 8 (2) (1989) 170 - 186.
- [7] G. N. Nurick and A. M. Radford, Deformation and tearing of clamped circular plates subjected to localised central blast loads, Recent developments in computational and applied mechanics: a volume in honour of John B. Martin, International centre for numerical methods in engineering (CIMNE), Barcelona, Spain (1997) 276-301.
- [8] S. Chung Kim Yuen and G. N. Nurick, The significance of the thickness of a plate when subjected to localised blast loads. *Proc 16th Int Symp Military Aspects of Blast and Shock* (MABS16), Oxford, UK (2000) 491-499.
- [9] R. G. Teeling-Smith and G. N. Nurick, The deformation and tearing of circular plates subjected to impulsive loads, *Int. J. Impact Eng.*, 11 (1) (1991) 77-92.
- [10] N. Jacob, G. N. Nurick and G. S. Langdon, The effect of stand-off distance on the failure of fully clamped circular mild steel plates subjected to blast loads, *Int. J. Engineering Structures*, 29 (2007) 2723-2736.
- [11] S. B. Menkes and H. J. Opat, Tearing and shear failure in explosively loaded clamped beams. *Exp. Mech.*, 13 (1973) 480-486.
- [12] G. N. Nurick and G. C. Shave, The deformation and tearing of thin square plates subjected to impulsive loads - an experimental study. *Int. J. Impact Eng.*, 18 (1) (1996) 99-116.
- [13] V. H. Balden and G. N. Nurick, Numerical Simulation of the Post Failure Motion of Steel Plates subjected to Blast Loading. *Int. J. Impact Eng.*, 32 (1-4) (2005) 14-34.
- [14] Y. Chen, J. Zhang, Y. Wang and P. Tang, Non-linear transient analysis of a blast-loaded circular plateresting on non-viscous fluid. *Int. J. Pressure Vessels and Piping*, 82 (2005) 729-737.
- [15] H. M. Wen, T. Y. Reddy and S. R. Reid, Deformation and failure of clamped beams under low speed impact loading. *Int. Jnl. of Impact Eng.*, 16 (3) (1995) 435-454.
- [16] H. M. Wen, T. X. Yu and T. Y. Reddy, Failure maps of clamped beams under impulsive loading. *Mech. Struct. & Mach*, 23 (4) (1995) 353-372.
- [17] H. M. Wen, T. X. Yu and T. Y. Reddy. A note on the clamped circular plates under impulsive loading. *Mech. Struct. & Mach*, 23 (3) (1995) 331-342.
- [18] H. M. Wen, Deformation and tearing of clamped circular work-hardening plates under impulsive loading. *Int. Jnl. of Pressure Vessels and Piping*, 75 (1998) 67-73.
- [19] H. Gharababaei and A. Darvizeh. Experimental and ana-

- lytical investigation of large deformation of thin circular plates subjected to localized and uniform impulsive loading, *Int. J. Mechanics based design of structure and machines*, 38 (2) (2010) 171-189.
- [20] N. Jones, *Structural impact*. Cambridge: Cambridge University Press (1989).
- [21] Y. Guo, Z. Zhuang, X. Y. Li and Z. Chen, An investigation of the combined size and rate effects on the mechanical responses of FCC metals, *Int. Jnl. of Solids and Structures*, 44 (2007) 1180-1195.
- [22] S. R. Bodner and P. S. Symonds, Experiments on viscoplastic response of circular plates to impulsive loading. *Int. Jnl. of Mechanics and Physi. GN.cs of Solids*, 27 (1979) 91-113.
- [23] G. N. Nurick, A new technique measure the deflection-time history of a structure subjected to high strain rates. *Int. Jnl. of Impact Eng.*, 3 (1985) 17-26.
- [24] T. J. Cloete, N. Nurick and R. N. Palmer, The deformation and shear failure of peripherally clamped centrally supported blast loaded circular plates, *Int. Jnl. of Impact Eng.*, 32 (2005) 92-117.
- [25] H. Gharababaei, N. Nariman-zadeh and A. Darvizeh. A Simple Modelling Method for Deflection of Circular Plates under Impulsive Loading using Dimensionless Analysis and Singular Value Decomposition. *Int. J. Mechanics* (2009), accepted and Article in press.



Hashem Gharababaei received his M.Sc. and Ph.D. degree in Mechanical Engineering from Guilan University. He is currently academic staff in the Department of Mechanical Engineering of the University of Guilan. His research interests are modeling using neural networks and non-dimensional analyze and

in the field of Impact and Blast Dynamics, Material Properties at High Strain Rates, Metals and Composites.